

# Response of a hexagonal NaI(Tl) scintillation probe in the attenuated neutron radiation of 14.1 MeV neutron generator ING-27

V.M. Bystritsky<sup>1</sup>, D.N. Grozdanov<sup>1,2</sup>, Yu.N. Kopatch<sup>1</sup>,  
I.N. Ruskov<sup>1,2\*</sup>, V.R. Skoy<sup>1</sup>, A.O. Zontikov<sup>1</sup>, and I.Zh. Ivanov<sup>1,2</sup>

<sup>1)</sup> Joint Institute for Nuclear Research, Frank Laboratory of Neutron Physics, Joliot-Curie 6, 141980 Dubna, Russia

<sup>2)</sup> Institute for Nuclear Research and Nuclear Energy, 72 Tzarigradsko chaussee Blvd., 1784 Sofia, Bulgaria

---

## Abstract

The experimental investigations of the 14.1 MeV neutron induced nuclear reactions, (n, n), (n, n'γ), (n, 2n), (n, f) and (n, γf) on a number of important for neutron-nuclear physics nuclei are the first priority scientific research in the frame of the new project TANGRA (Tagged Neutrons & Gamma Rays) [1], which has been recently started at Frank Laboratory of Neutron Physics of the Joint Institute for Nuclear Research in Dubna, Russia. Since the neutron and gamma yields from these reactions are quite small the background conditions become an important issue. A number of experiments were done to find the optimal type and size of the shielding for the TANGRA setup neutron and gamma detectors against the transmitted and scattered (n+γ)-radiation. To protect a hexagonal NaI(Tl) scintillation gamma-ray spectrometric probe from the direct radiation of the sealed-tube portable neutron generator ING-27, which was used as a 4π “point source” of 14.1 MeV neutrons, a set of homogeneous and composite shields of different length and materials were tested. Here the results from these experiments are reported and discussed.

© 2016 The Authors. JINR Publishing Office.

Keywords: Gama-ray spectrometry, NaI(Tl), Tagged neutron method, ING-27, TANGRA-setup

---

\* Corresponding author: I.N. Ruskov, tel. +7 (496216) 2785  
e-mail: ruskoiv@nf.jinr.ru

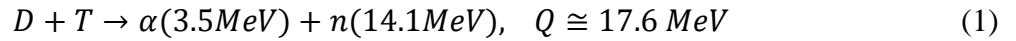
## 1. Introduction.

To study some important for fundamental and applied nuclear physics reactions (n,n), (n,n'γ), (n,2n), (n,f), (n,γf), induced by 14.1 MeV neutrons, TANGRA-project has been recently started in Frank Laboratory of Neutron Physics (FLNP) of the Joint Institute for Nuclear Research (JINR) in Dubna, Russian federation [1].

Since the yield of this type of reactions is small, one is generally faced with the problem of suppressing the neutron-gamma “background”, produced by neutrons that penetrate directly from the source (or scattered on the environmental materials) in the scintillation detectors that are used to detect secondary nuclear radiation (neutrons and gamma-rays).

Some methodological work has been done to optimized the TANGRA (Tagged Neutrons & Gamma Rays) experimental setup geometry (Fig. 1) [2], for investigation of the angular anisotropy of the irradiated gamma-rays from the inelastic scattering of 14.1 MeV neutrons in carbon.

As a source of neutrons a VNIIA portable neutron generator ING-27 (Fig. 1, 1) is used [3]. The 14.1 MeV neutrons are produced in D-T fusion-fission reaction:



The incorporated in ING-27 vacuum chamber 64-pixel  $\alpha$ -particle sensor permits to “tag” and count every neutron, because the both reaction products are irradiated nearly collinear in opposite directions.

The main advantages of the sealed-tube are a) it eliminates the use of a vacuum pump and b) ensure the safety of the radioactive tritium.

For detection of the characteristic gamma-rays from the inelastic scattering of 14.1 MeV neutrons in the target samples, 22 Amcryst<sup>®</sup> hexagonal NaI(Tl) probes (Fig.1, 3) from “Romashka” setup [4] were arranged vertically on a horizontal ring of an internal diameter of  $\sim 62$  cm.

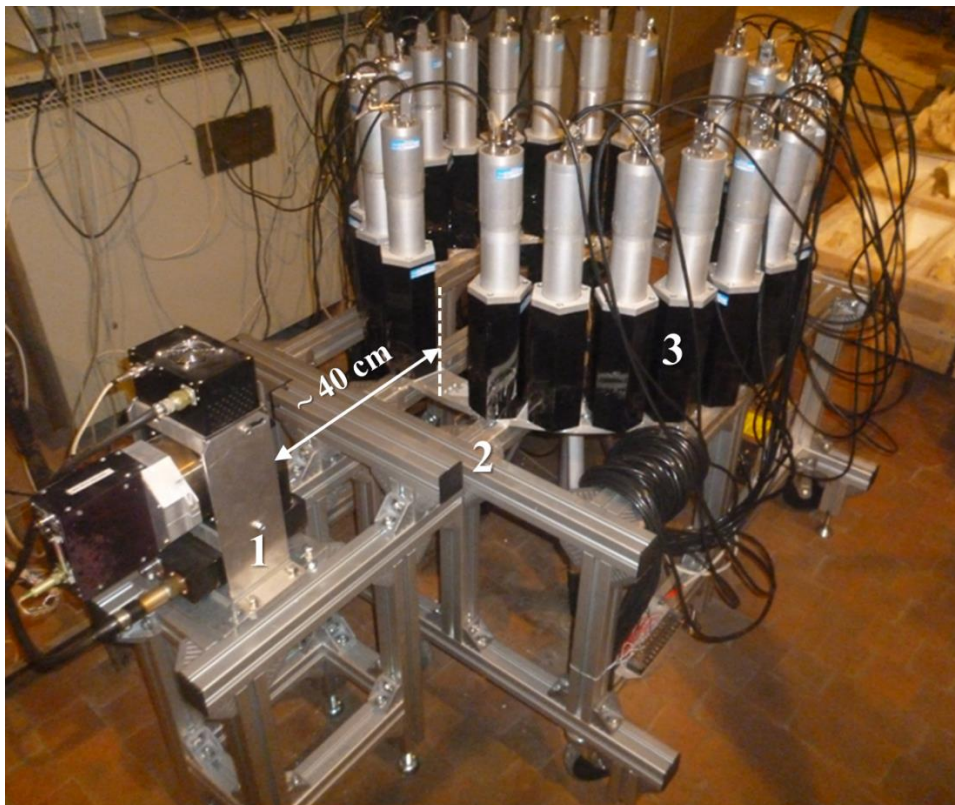


Fig. 1. Base TANGRA Setup: 1 – portable sealed-tube 14.1 MeV neutron generator ING-27, 2 – aluminum support, 3 – 22 hexagonal NaI(Tl) scintillation gamma-ray spectrometer. The size is in (cm).

The NaI(Tl) scintillator material has the light yield of  $\sim 38$  photons/keV,  $1/e$  decay time of  $\sim 250$  ns, and density of  $\sim 3.67$  g/cm<sup>3</sup>. Atomic numbers are 53 and 11 for iodine and sodium, respectively. Under neutron irradiation, the NaI(Tl) scintillator is activated by neutrons showing the delayed beta decay spectral continuum with the endpoint energy of  $\sim 2$  MeV.

Neutron- and gamma- radiation shielding materials has been always an interesting research area in nuclear, radiation physics and radiation protection.

To shield 14 MeV neutrons there is no good shielding material, because the absorption cross sections is very small. For example, the shielding calculations show that the flux of 14 MeV

neutrons is reduced by a factor of 10 for each 37.5 cm of solid concrete block. Therefore, a 152 cm thick concrete block will reduce the neutron flux to approximately 9 neutrons/cm.sec<sup>2</sup>, which is within the radiation protection permissible level. For extra shielding, concrete walls of ~200 cm thickness are often used. Generally speaking, in order to have a good shielding the mean free path of neutron in the material should be small.

In heavy elements like tungsten (W) and lead (Pb) there are two dominant reactions at 14 MeV namely elastic scattering (n, n), (n, 2n) reaction, the cross sections of which are relatively high. One can use the (n, 2n) reaction to produce more neutrons with lower energies. The typical energy of the out coming neutrons from the (n, 2n) reaction ranges from 0.5 MeV to 1.5 MeV.

Because the neutron multiplication depends upon the thickness of the shielding, the different layers in composite shielding materials can be optimized using Monte Carlo simulation technics realized in a number of computer software packages like MCNP, FLUKA, GEANT.

These neutrons should be slowed down further on, so one can use a material with a large inelastic scattering cross section to slow down the neutrons.

So, the third mechanism is the inelastic neutron scattering (INS), denoted as (n, n'γ), with a threshold energy of ~850 keV. Here, fast neutrons are inelastic scattered for example from iron (Fe) or steel, inducing gamma-ray emission from the 846 keV level. This reaction has a 10-fold higher cross-section than the (n, p) one (Table 1). During the inelastic process a number of characteristic gamma rays are irradiated.

Table 1. Nuclear data for threshold reactions of 14 MeV Neutrons on Iron (Fe).

Reaction	Isotope Abundance (%)	Cross Sections (b)	Half-life (min)	Gamma Energy (keV)	Gamma Yield
<sup>54</sup> Fe(n,2n) <sup>53</sup> Fe	5.84	0.015	8.5	511	1.96
<sup>56</sup> Fe(n, p) <sup>56</sup> Mn	91.68	0.103	154.56	847	0.99
				1810	0.29
				2110	0.15
<sup>57</sup> Fe(n, p) <sup>57</sup> Mn	2.17	0.060	1.7	120	1
				130	1
<sup>56</sup> Fe(n,n'γ) <sup>56</sup> Fe	91.68	~ 1	Prompt	847	0.99

So, layers of heavy elements, such as iron (Fe), placed within a hydrogenous medium as water (H<sub>2</sub>O), paraffin wax (C<sub>25</sub>H<sub>52</sub>), polyethylene (C<sub>2</sub>H<sub>4</sub>), can remove very efficiently the fast neutrons. Iron (Fe) also shields the gamma-rays produced by inelastic scatter and neutron capture within the vault or shielding. The problem of these secondary gamma-rays produced due to neutron interactions with Fe is solved with higher material thickness, where there is an exponential relation between the number of the secondary gammas and the material thickness due to the material self-shielding. On the other side, gamma-ray build-up factors are geometry dependent, which correct the attenuation calculations for poly-chromatic rays, thick absorbing material and wide beam geometries (as of TANGRA setup).

Once the neutrons are slowed, they must be absorbed by a neutron absorber. Boron (<sup>10</sup>B) has a high cross section for capturing thermal neutrons. Borated polyethylene (BPE) or borated high-

density polyethylene (BHDPE) can be placed on the outside of the shield, so after being slowed down to thermal energy, the neutrons can be captured by boron. The main characteristics of the most common used fast neutron shielding materials are briefly listed in Table 2.

That is why becomes important the passive shielding, designed for protection of scintillation detectors from the neutrons coming directly from the source, to be optimized by computer simulations and/or measurements.

Table 2. The main characteristics of some materials used in fast neutron shielding.

Shielding material	Density, g/cm <sup>3</sup>	Melting point, °C	Protection		Known drawbacks
			Gamma Rays	Fast neutrons	
Depleted natural Uranium (0.2% of <sup>235</sup> U)	19	1133	excellent	Bad, Undergo fission	Oxidize, Pyrophoric, Difficult to machine.
Lead (Pb)	11.3	327.6	Very good	Good	Chemically toxic, Low melting point.
Bismuth (Bi)	9.7		Good	Good	Radio-toxic
Tungsten (W)	19.3	3410	Good	Good	Expensive, Difficult to machine.
Hevimet alloy HD18, 95%W+3.5%Ni+1.5%Cu	18		Good	Good	Expensive
Iron (Fe)	7		Good	Good	Oxidize
Pure Polyethylene (PE) (CH <sub>2</sub> ) <sub>n</sub>	0.92	82	Not good	Good	Flammable, Radiation non-resistant. $\sigma(^1\text{H}(n,\gamma)^2\text{H}) = 0.33 \text{ b}$ @ $E_n = 0.027 \text{ eV}$ , $E_\gamma = 2.2 \text{ MeV}$
Borated Polyethylene (BPE) (CH <sub>2</sub> ) <sub>n</sub> , Boron 10% wt	0.96-0.97		Not good	Very good	Flammable, Radiation non-resistant. $\sigma(^{10}\text{B}(n,\alpha)^7\text{Li}) = 3837 \text{ b}$ @ $E_n = 0.027 \text{ eV}$ , $E_\gamma = 0.478 \text{ MeV}$ (94%)

The objective of this study was to investigate the shielding effectiveness of different combination of layers from lead (Pb), iron (Fe), polyethylene (PE) and/or borated polyethylene (BPE).

The goal of the experimental study was to obtain the best ratio of the benefit/cost combination of the materials, which can provide a reasonable protection of a NaI(Tl) scintillation gamma-ray detector from the direct neutron beam of the ING-27 neutron generator. In the same time some addition constrains were put on the shielding characteristics, as: shield should a) not to be thicker than 50 cm b) not be heavy c) be easily accessible for handling d) not become so strongly activated that to present health hazards.

## 2. Experimental setup. Data acquisition and reduction.

The measurements were carried out in environmental conditions very close to those where we suppose to dislocate the TANGRA setup.

The passive shields, composed from layers of different materials, was positioned between the neutron generator ING-27 and the investigated hexagonal NaI(Tl) scintillation probe as shown in Fig. 2. The distance between the output “window” of the neutron generator ING-27 and the NaI(Tl) gamma-ray detector frond-end was  $\approx 61 \text{ cm}$  and remained unchanged for all types of shielding configurations. The distance between the output “window” of the neutron generator and the

shielding front surface was  $\approx 7$  cm and remained unchanged even when the shielding thickness and the combinations of different type of layers that constitute this shielding were varied.

The objective of the study was to investigate the shielding effectiveness of different combination of lead (Pb), iron (Fe), polyethylene (PE) and/or borated polyethylene (BPE) plates.

The signals from the ING-27  $\alpha$ -detector processing and NaI(Tl) probe were collected and analyzed by TANGRA DAQ – a computerized 32-channel digital readout system, utilizing two ADCM16-LTC (16-channel/14-bit/100MHz) ADC-boards from AFI Electronics<sup>®</sup> described in details somewhere else [2, 4].

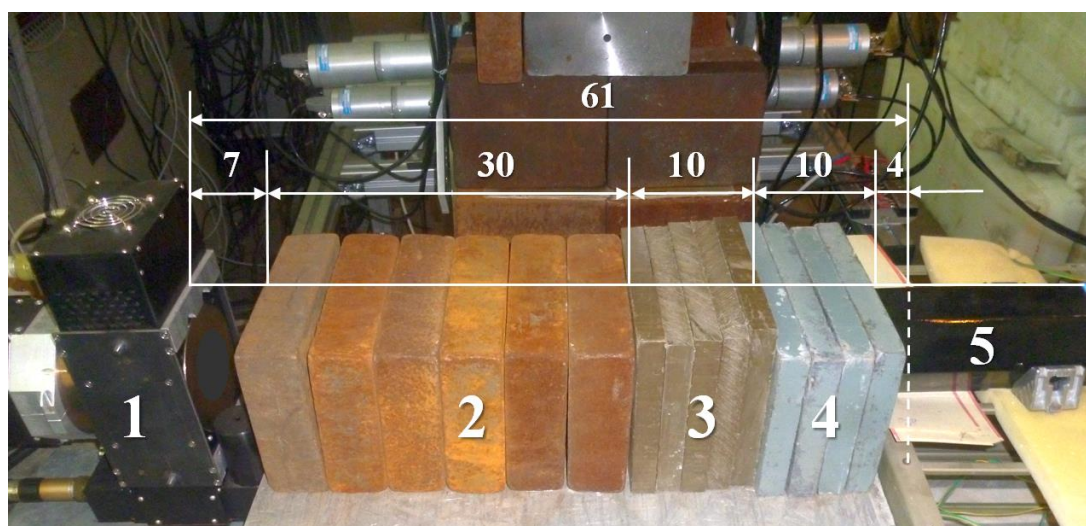


Fig. 2. The experimental arrangement: 1– portable sealed-tube 14.1 MeV neutron generator ING-27, 2 – Fe, 3– BPE, 4 – Pb, 5 – hexagonal NaI(Tl) scintillation gamma-ray spectrometer. The sizes are in (cm).

In all the measurements, the neutron flux incident on the NaI(Tl) (shield) was monitored, registering the  $\alpha$ -particles formed in reaction (1) by the embedded Si  $\alpha$ -particle detector.

NaI(Tl) count-rate suppression factor  $f$  was defined as a ratio of the number of events recorded by the bare NaI(Tl),  $N_0$ , and those of the shielded one,  $N_d$ , i.e.

$$f = N_0/N_d \quad (2)$$

Number of events  $N_0$  and  $N_d$  was determined from the corresponding gamma-ray pulse-height spectra (number of events per amplitude channel) as a function of the light output (LO) of the NaI(Tl) scintillator in MeVee units (equivalent to 1 MeV electron light output) (Figs. 3-5). Some spectra were truncated rejecting (discriminating) the gamma-ray events with light output bellow  $\sim 0.2$  MeVee (Figs. 3-5).

All the spectra are formed by a) neutrons which traversed the shielding or b) scattered by it (surrounding) materials then entered NaI(Tl), and c)  $\gamma$ -quanta from the interaction of neutrons with the shielding (surrounding) materials registered by NaI(Tl).

The results from the investigation of the shielding properties of Pb, Fe, and BPE (and their combination) in the mixed neutron/gamma field, caused by 14.1 MeV neutrons, are following.

### 3. Experimental results.

In Fig. 3. are shown the amplitude distributions of events recorded by NaI(Tl) probe located behind 10, 20, 50 cm thick Fe shield, compare with that of the bare probe, in the interval of  $2.0 \div 6.9$  MeVee. It is seen that 40–50 cm thick Fe shield reduced the loading of NaI(Tl) more than 4 times in the region of its  $\sim 4.4$  MeVee light output, where is expected to appear the peak of 4.44 MeV gamma-rays arising from the inelastic scattering of 14.1 MeV neutrons on  $^{12}\text{C}$  nuclei.

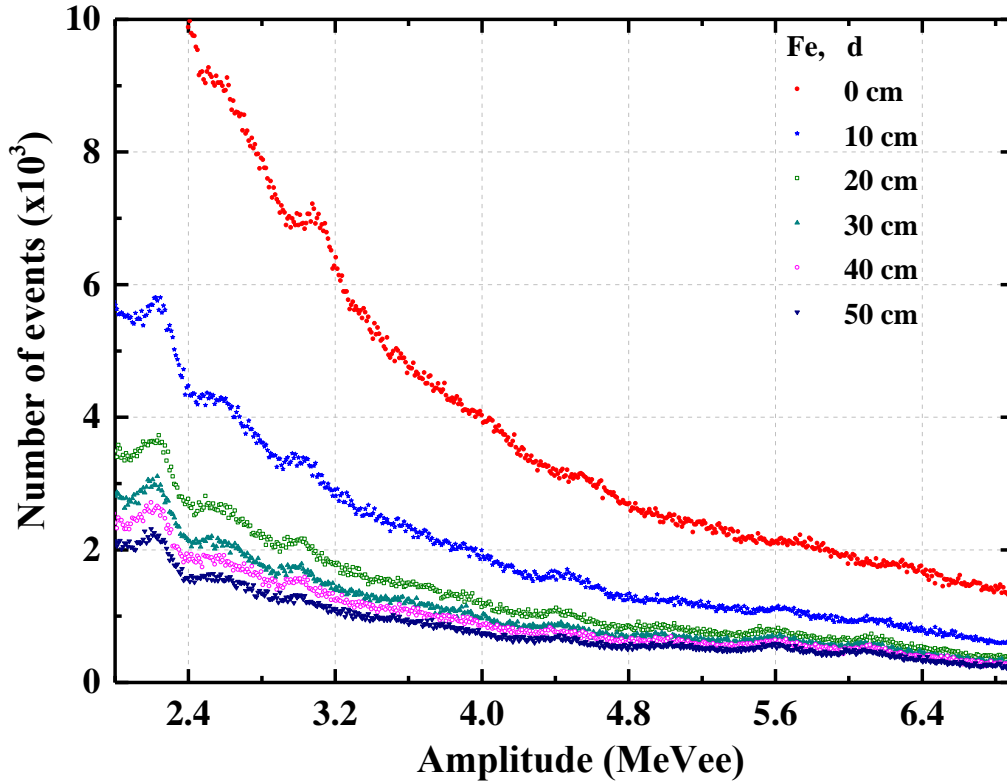


Fig. 3. Amplitude distributions of events recorded by NaI(Tl) probe located behind 10, 20, 30, 40 and 50 cm thick Fe shields, compare with that of the bare probe, in the NaI(Tl) scintillator light output interval of  $\text{LO} = 2.0 \div 6.9$  MeVee.

In Fig. 4 and Fig. 5 are shown the amplitude distributions of events recorded by NaI(Tl) probe located behind 50 cm thick Fe (open squares) and Pb (full circles) shields, in the interval of  $\text{LO} = 0.2 \div 6.9$  MeVee. It is seen that there are some deviations in the NaI(Tl) light output region below 2-3 MeVee. In the higher region no significant deviations found.

The determined NaI(Tl) count-rate suppression factors  $f$  for used Fe and Pb shield thicknesses are listed in Table 3. In all the tables and graphs, the error bars indicate the total data uncertainties if not specially specified.

In Fig. 8 is shown NaI(Tl) load suppression factors  $f$  as a function of Fe\* and Pb\* uniform shield thickness  $d = 0 \div 50$  cm (\* – indicates that the thickness of the layer varied). It is seen that the load on NaI(Tl) probe is reducing  $\sim (1.8 \div 3.8)$  times when using (10  $\div$  50) cm thick shields of Fe (or Pb) and the difference between the both type of shielding is  $< 7\%$  (Table 3).

In Table 4 are shown NaI(Tl) load suppression factors  $f$  as a function of the thickness  $d$  of Fe\* and Pb\* layers in the combine (composite) 50 cm thick (Fe\* + Pb\*) shields.

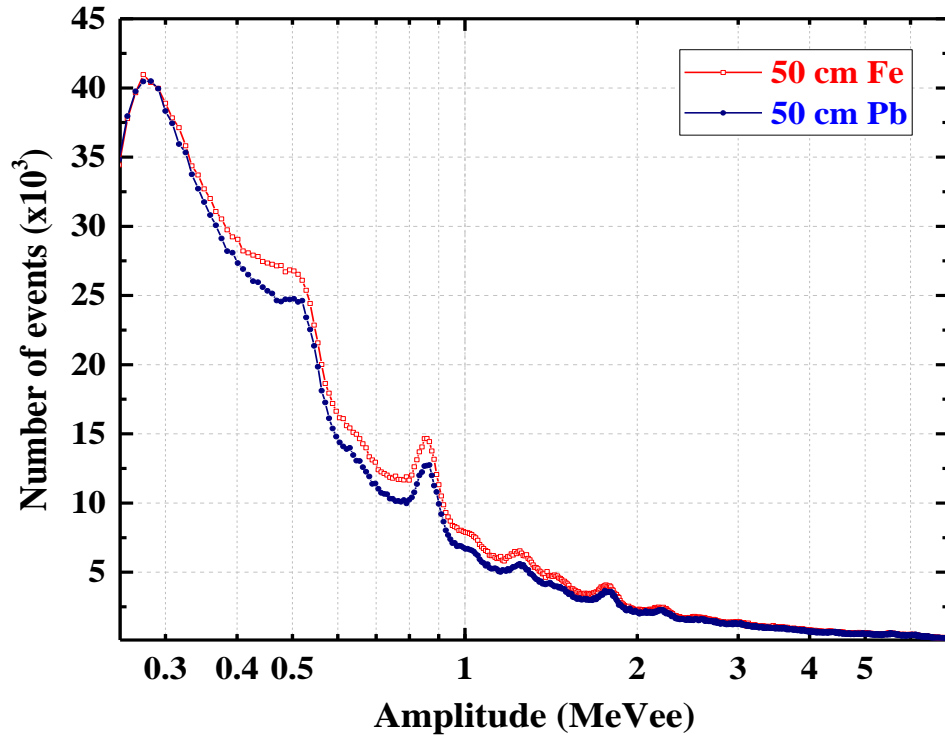


Fig. 4. Amplitude distributions of events recorded by NaI(Tl) probe behind 50 cm thick Fe and Pb shields in the interval of  $LO = 0.2 \div 6.9$  MeVee.

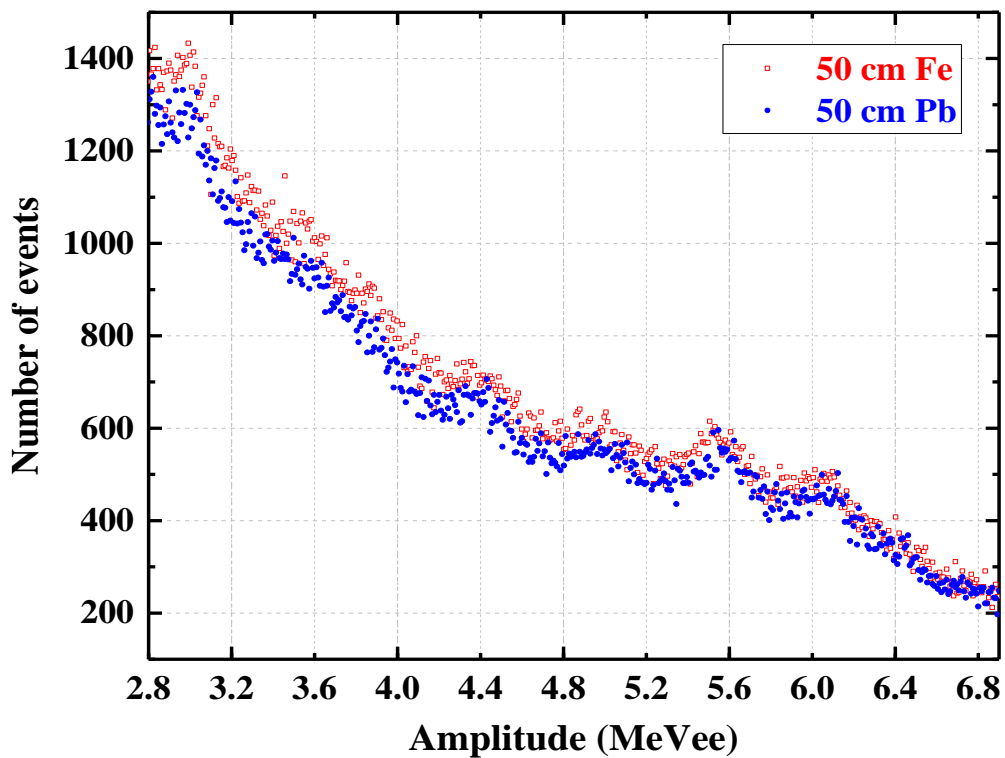


Fig. 5. Amplitude distributions of events recorded by NaI(Tl) probe behind 50 cm thick Fe and Pb shields in the interval of  $LO = 2.8 \div 6.9$  MeVee. The lowest light output limit was  $LO = 0.2$  MeVee.

Table 3. NaI(Tl) load suppression factors  $f$  as a function of the thickness  $d = (10 \div 50)$  cm of the uniform shields made of Fe\* and Pb\* layers.

d, cm	0	10	20	30	40	50
$f(d_{\text{Fe}^*})$	1	$1.77 \pm 0.10$	$2.54 \pm 0.10$	$2.96 \pm 0.10$	$3.27 \pm 0.10$	$3.84 \pm 0.10$
$f(d_{\text{Pb}^*})$	1	$1.83 \pm 0.10$	$2.37 \pm 0.10$	$2.81 \pm 0.10$	$3.12 \pm 0.10$	$3.74 \pm 0.10$
$\Delta f, \%$		-3.4	6.7	5.1	4.6	2.6

Table 4. NaI(Tl) load suppression factors  $f$  as a function of the thickness  $d$  of Fe\* and Pb\* layers in composite 50 cm thick (Fe\* + Pb\*) shields.

$d_{\text{Fe}^*}+d_{\text{Pb}^*}$ , cm	0+50	10+40	20+30	30+20	40+10	50+0
$f(d_{\text{Fe}^*}+d_{\text{Pb}^*})$	$3.6 \pm 0.1$	$3.6 \pm 0.1$	$3.57 \pm 0.1$	$3.6 \pm 0.1$	$3.6 \pm 0.1$	$3.9 \pm 0.1$
$d_{\text{Pb}^*}+d_{\text{Fe}^*}$ , cm	0+50	10+40	20+30	30+20	40+10	50+0
$f(d_{\text{Pb}^*}+d_{\text{Fe}^*})$	$3.7 \pm 0.1$	$4.0 \pm 0.1$	$3.9 \pm 0.1$	$3.9 \pm 0.1$	$4.0 \pm 0.1$	$3.6 \pm 0.1$
$\Delta f, \%$	-3.1	11.8	-8.7	-7.5	-8.5	8.0

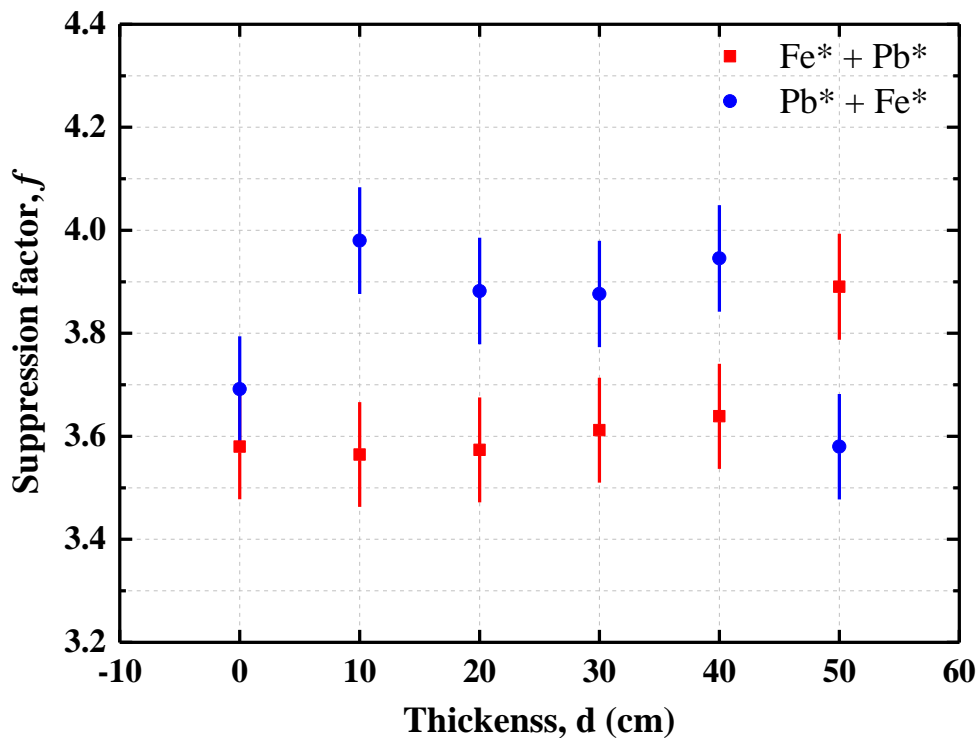


Fig. 6. NaI(Tl) load suppression factors  $f$  as a function of the thickness  $d$  of Fe and Pb layers in composite 50 cm thick (Fe\* + Pb\*) and (Pb\* + Fe\*) shields.

From Table 4 and Fig. 6 is seen that two-component (Fe\*+Pb\*) or (Pb\*+Fe\*) composite metal shields differ in suppressing the NaI(Tl) load by < 12%.

Mixed metal, H- and B- containing materials (water, paraffin wax, polyethylene) has been used in a good number of experimental and simulation studies. The results from such studies can be

found in refs. 6–13. The main idea is to reduce the size of the shielding, attenuate as much as possible the radiation at the place of the detector systems.

We investigated one 2-layer 50 cm thick composite shield made of Fe(40cm) + BPE(10cm) and three 3-layer composite 50 cm thick shields with variable thickness of Fe (30, 20, 10 cm) and Pb (10, 20, 30 cm) layers, correspondingly, while the BPE layer between them was 10 cm thick.

In Fig. 7 are shown the amplitude spectra of events recorded by NaI(Tl) probe behind 50 cm thick composite Fe\*+BPE(10cm)+Pb\* shields with  $d_{Fe^*} = (10 \div 40)$  cm and  $d_{Pb^*} = (30 \div 0)$  cm, in the interval of LO = 2.8 ÷ 6.9 MeVee. The lowest NaI(Tl) probe LO-limit was set to 0.2 MeVee.

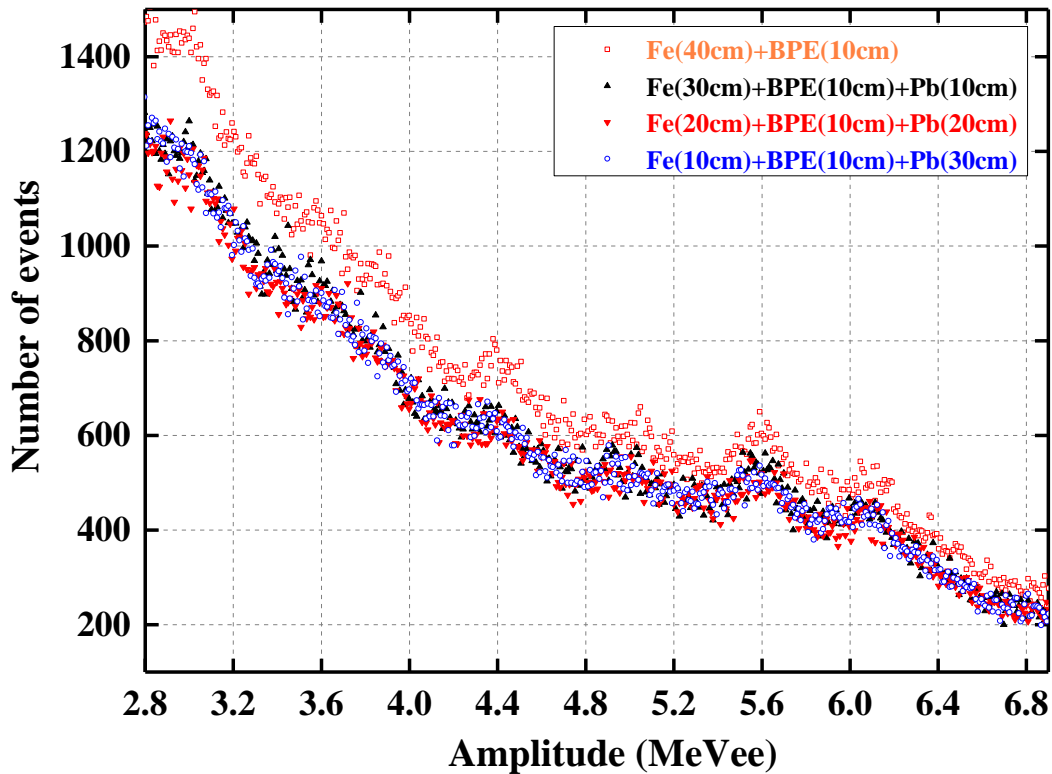


Fig. 7. Amplitude spectra of events recorded by NaI(Tl) probe behind 50 cm thick composite (Fe\*+BPE+Pb\*) shields in the interval of LO = 2.8 ÷ 6.9 MeVee.

In Table 5 and Fig. 8 are shown the dependence of the count-rate suppression factors  $f$  of the NaI(Tl) detector behind 50 cm thick composite Fe\*+BPE(10cm)+Pb\* shields with  $d_{Fe^*} = (10 \div 40)$  cm and  $d_{Pb^*} = (30 \div 0)$  cm.

Table 5. NaI(Tl) load suppression factor  $f$  as a function of the thickness  $d$  of Fe\* and Pb\* layers in the combined 50 cm thick Fe\*+BPE(10cm)+Pb\* shield.

$d_{Fe^*}+d_{BPE}+d_{Pb^*}$ , cm	10+10+30	20+10+20	30+10+10	40+10+0
$f(d_{Fe^*}+d_{BPE}+d_{Pb^*})$	$4.08 \pm 0.10$	$4.21 \pm 0.10$	$4.09 \pm 0.10$	$3.38 \pm 0.10$

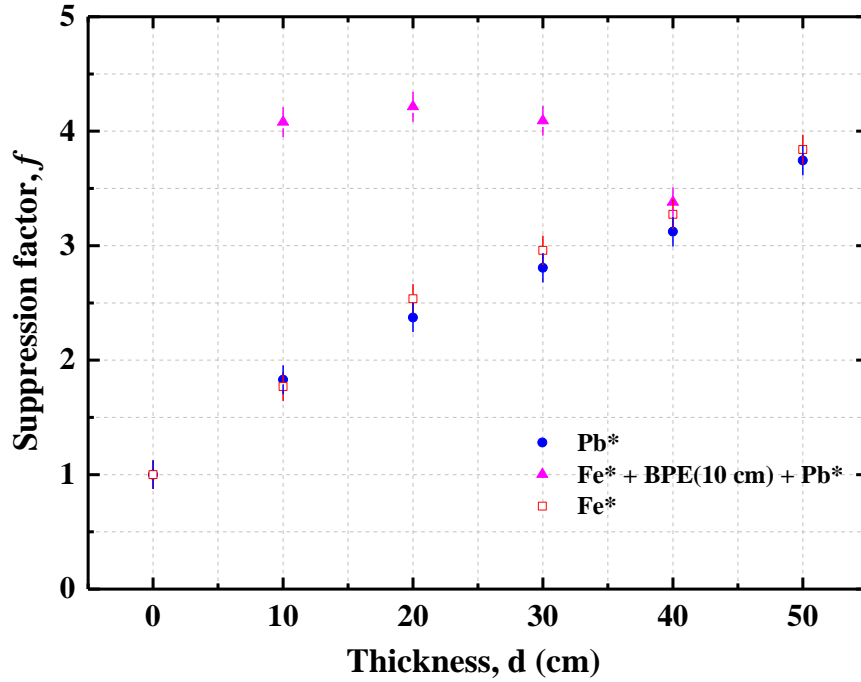


Fig. 8. NaI(Tl) load suppression factor  $f$  as a function of  $\text{Fe}^*$  and  $\text{Pb}^*$  uniform shield thickness  $d$  together with that of the combined 50 cm thick  $\text{Fe}^* + \text{BPE}(10\text{cm}) + \text{Pb}^*$  shield with variable (\*) thickness of Fe and Pb layers.

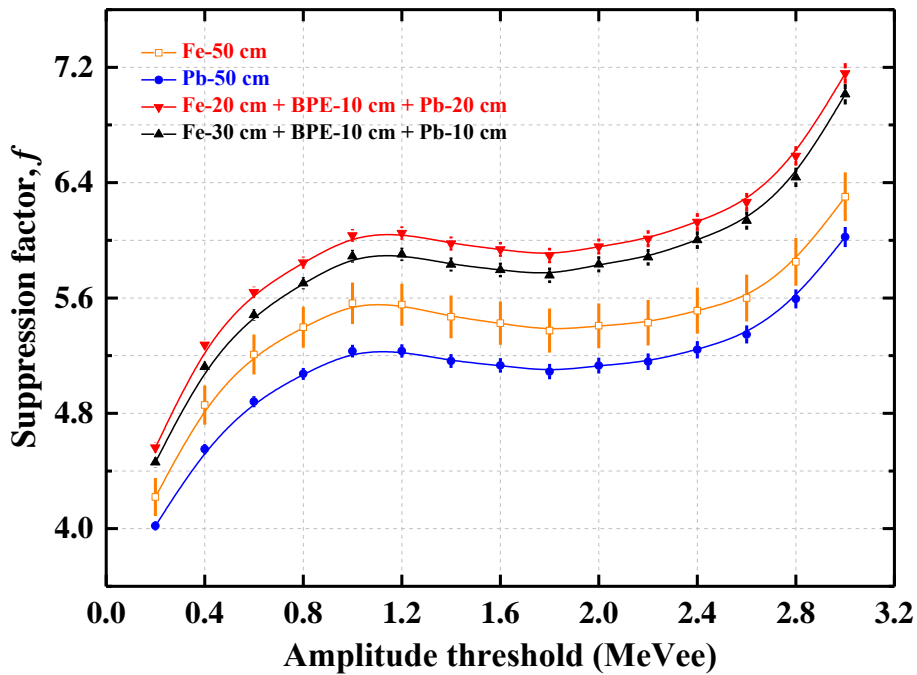


Fig. 9. Dependence of NaI(Tl)  $\gamma$ -ray detector load suppression factors behind a 50 cm thick Fe, Pb, composite Fe(20cm)+BPE(10cm)+Pb(20cm) and Fe(30cm)+ BPE(10cm)+Pb(10cm) shields on its light output threshold level. The minimum LO-threshold was 0.2 MeVee. The error bars shown for Fe-data indicate the total uncertainties, for those of the other data only the statistical uncertainties are shown for lucidity.

From Fig.7 and Fig. 8 one can conclude that a) in the presents of BPE it is important to have additional heavy metal shield before NaI(Tl) to suppress gamma-rays from the interaction of the moderated (by Fe) neutrons with the BPE-nuclei and b) in the case of triple-layer shields, the complementary thicknesses of Fe and Pb shown the same level of suppression in the range of experimental data uncertainties.

In Fig. 9 are shown the dependence of NaI(Tl) gamma-ray detector load suppression factors behind a 50 cm thick Fe, Pb, composite Fe (20 cm) + BPE(10 cm) + Pb(20 cm) and Fe (30 cm) + BPE (10 cm) + Pb (10 cm) shields on its light output threshold level. The minimum light output chosen was  $LO = 0.2 \text{ MeVee}$ . It can be seen that NaI(Tl) count rate suppression factor, behind the composite Fe(20cm)+BPE(10cm)+Pb(20cm) or Fe(30cm)+BPE(10cm)+Pb(10cm) shield and for a light output threshold in the range of  $0.2 \div 3.00 \text{ MeVee}$ , is increased by  $\sim 10\%$  with respect to the similar values measured with 50 cm thick Fe or Pb shields.

#### 4. Discussion and conclusions.

In the frame of TANGRA-project some experimental work was done in order to choose the optimum type and thickness of a shadow radiation shielding to protect a NaI(Tl) scintillation gamma-ray detector from ING-27 direct 14.1 MeV neutrons.

A shielding is required to protect the gamma-ray detector from direct hit by the neutrons and produced by them gamma-radiation. The size of the shielding defines the geometry of the experimental setup since the neutron source and the gamma-ray detector are separated by it.

The goal is to keep the fast neutrons away from the detector volume either by redirecting their path (via elastic or inelastic scattering) or moderating them with the subsequent capture.

Because ING-27 D-T target is of a “point source” type, the shielding may have a conical shape to minimize its weight, but because in the present methodological experiments this was not of importance, parallelepiped bricks of different materials (Fe, BPE, Pb) were used.

As a rule, a combination of materials with large scattering cross sections for fast neutrons and large low energy neutron capture cross sections, and high Z materials with high stopping power for gamma-rays is used.

For a  $10^7 \text{ n/s}$  D-T source like ING-27, the simplest “shadow” shielding can be a layered conical structure of  $\sim 40 \div 50 \text{ cm}$  thickness (length), for example, a  $30 \div 40 \text{ cm}$  BPE layer (or  $10 \div 30 \text{ cm}$  Fe+10cm BPE) near the source, and a  $10 \div 20 \text{ cm}$  Pb-layer near the NaI(Tl) gamma-ray detector. Of course, more complex shielding designs are possible using layers of other materials (concrete, depleted uranium, bismuth, (borated) paraffin vax, water, resin, etc.), but the size-weight-cost considerations can add some limitations.

In addition, the NaI(Tl) gamma-detector may be also shielded from lower energy neutrons scattered from surrounding materials. A two-layer shielding can reduce spectral “noise” due to low energy neutron interactions with the detector crystal. An outer layer of borated resin or BPE is effective as a thermal neutron shielding, an inner Pb-layer attenuates photons emitted from thermal neutron capture reactions in the outer layer, as well as the low energy photons that are not of interest in material science analysis, thus helping to reduce the dead time of the NaI(Tl) gamma-ray spectroscopy system.

However, a shield with both Fe and BPE could be more effective than just Fe or BPE alone, because the advantages of both Fe and BPE are utilized. Iron (Fe) is effective in slowing down

high-energy neutrons (e.g., 14-MeV source neutrons) and attenuating gammas, while hydrogen of BPE is effective in slowing down fast neutrons (till a few MeV), and  $^{10}\text{B}$  has a high absorption cross section for thermal neutrons and a low production yield of gammas. So, a shield made of 30cm Fe followed by a 20 cm BPE-layer can meet the goal.

According to the experimental results obtained in this methodological work, three layer shields made of Fe(30cm)+BPE(10cm)+Pb(10cm) or Fe(20cm)+BPE(10cm)+Pb(20cm) provided the highest suppression factors on the hexagonal NaI(Tl) gamma-ray detector load.

Some data and results from the similar experimental investigations with neutron and gamma-ray detectors based on BGO and Stilbene crystals will be published somewhere else [14].

## Acknowledgements

This work was partially supported by a Grant of the Plenipotentiary Representative of Republic of Bulgaria in JINR.

## References

1. Yu. N. Kopatch, V.M. Bystritsky, et. al, "Development of the tagged neutron method for elemental analysis and nuclear reaction studies (project TANGRA)", 22nd International Seminar on Interaction of Neutrons with Nuclei, ISINN-22, 2014, Dubna, Russia, [http://isinn.jinr.ru/past\\_isinns/isinn\\_22/progr128\\_05\\_2014/Kopatch.pdf](http://isinn.jinr.ru/past_isinns/isinn_22/progr128_05_2014/Kopatch.pdf).
2. I.N. Ruskov, Yu.N. Kopatch, V.M. Bystritsky et al., TANGRA-Setup for the Investigation of Nuclear Fission induced by 14.1 MeV neutrons, *Physics Procedia* **64** (2015)163-170; ISSN - 23:1875-3892, <http://dx.doi.org/10.1016/j.phpro.2015.04.022>.
3. Neutron Generators for Analysis of Substances and Materials. ING-27 gas-filled neutron tube based neutron generator of VNIIA, [http://www.vniia.ru/eng/ng/docs/ing\\_element\\_eng.pdf](http://www.vniia.ru/eng/ng/docs/ing_element_eng.pdf).
4. V.R. Skoy, Yu.N. Kopatch, I. Ruskov, et al., A versatile multi-detector gamma-ray spectrometry system for investigation of neutron induced reactions, *Proc. of ISINN-21*, 2013, <http://isinn.jinr.ru/proceedings/isinn-21/pdf/ruskov.pdf>.
5. V.M. Bystritsky et al. "Gamma detectors in explosives and narcotics detection systems," *Phys. Part. Nucl. Lett.* **10** (2013) 566-572.
6. T. Maruyama, C. J. Bouts, Attenuation of 15 MeV neutrons in multilayer shields composed of steel, polyethylene and borated materials, *Med. Biol.* **17** (1972) 420, <http://iopscience.iop.org/article/10.1088/0031-9155/17/3/010/pdf>.
7. Gad Shani, Iron-water combination for shielding of 14 MeV neutrons, *Annals of Nuclear Energy* **4/2-3**, 1977, Pages 65-67, [http://dx.doi.org/10.1016/0306-4549\(77\)90003-2](http://dx.doi.org/10.1016/0306-4549(77)90003-2).
8. J.J. Broerse, A.C. Engels, J.S. Groen, Production and shielding of 15 MeV neutrons, *European Journal of Cancer* **7/ 2-3** (1971) 105-114, [http://dx.doi.org/10.1016/0014-2964\(71\)90003-X](http://dx.doi.org/10.1016/0014-2964(71)90003-X).
9. Marion L. Stelts, Sam Donaldson, Jeanetta Povelites, Transport of 14 MeV and fission spectrum neutrons through spheres — an aid to shielding design, *Nucl. Instr. Meth.* **187/2-3** (1981) 483-488, [http://dx.doi.org/10.1016/0029-554X\(81\)90377-3](http://dx.doi.org/10.1016/0029-554X(81)90377-3).
10. L. Wielopolski, S. Mitra, O. Doron, Non-carbon-based compact shadow shielding for 14 MeV neutrons, *Journal of Radioanalytical and Nuclear Chemistry* **276/1** (2008) 179-182, [http://dx.doi.org/10.1016/0014-2964\(71\)90003-X10.1007/s10967-007-0429-1](http://dx.doi.org/10.1016/0014-2964(71)90003-X10.1007/s10967-007-0429-1).

11. Abbas J. Al-saadi, Iron-Polyethylene Combination for Shielding of 14 MeV Neutrons, *Journal of Kufa – Physics* **2/1** (2010) 1-3,  
<http://www.uokufa.edu.iq/journals/index.php/jkp/article/view/1338/1202>.
12. Majid Zarezadeh, The Preparation of Polyethylene and Mineral Material Composites, and Experimental and Theoretical (using MCNP Code) Verification of their Characteristics for Neutron Beam Attenuation, *Journal of Science and Engineering* **1/2** (2013) 95-101,  
<http://www.oricpub.com/SE-1-2-28-1.pdf>.
13. Lan Min, Zhang Jingjie, Cheng Daowen, 14 MeV Neutron Shielding Material Designed by MCNP Code, *Journal of Jilin University Science Edition* **53/2** (2015) 316-319,  
<http://xuebao.jlu.edu.cn/lxb/EN/Y2015/V53/I02/316#>.
14. V. M. Bystritsky, V. Valkovic, D.N. Grozdanov, A.O. Zontikov, I.Zh. Ivanov, Yu. N. Kopatch, A. R. Krylov, Yu. N. Rogov, I. N. Ruskov, M.G. Sapozhnikov, V.R. Skoy, V.N. Shvetsov, Multilayer passive shielding of scintillation detectors based on BGO, NaI(Tl), and stilbene crystals operating in intense neutron fields with an energy of 14.1 MeV, *Physics of Particles and Nuclei Letters* **12/2** (2015) 325-335.